

## Thermal Characterisation of Self-Organised Helical States in RFX

P.Franz<sup>1,2</sup>, L.Marrelli<sup>1</sup>, P.Martin<sup>1,2</sup>, P.Nielsen<sup>1</sup>, R.Pasqualotto<sup>1</sup>, G.Spizzo<sup>1,2</sup>

<sup>1</sup>*Consorzio RFX – Corso Stati Uniti, 4 – 35127 Padova – Italy*

<sup>2</sup>*Istituto Nazionale di Fisica della Materia–UDR di Padova – Italy*

*e-mail: franz@igi.pd.cnr.it*

### 1. Introduction

Experiments in RFX [1], a large reversed field pinch (RFP) device with circular cross section (major radius  $R=2$  m, minor radius  $a=0.46$  m, target plasma current  $I=2$  MA), have shown the presence of a nested helical structure in the plasma core [2]. These states are obtained both transiently and in steady state as a result of plasma self-organisation: during such states, relatively large, bean-shaped,  $m=1$  structures in the Soft-X-Ray (SXR) emissivity profiles are observed. They are originated by a single ( $m=1, n=n_0$ ) magnetohydrodynamic (MHD) dynamo mode which dominates the  $m=1$  modes  $n$  spectrum: for this reason these states are dubbed Quasi Single Helicity (QSH) states. QSH differs from the standard RFP states, or Multiple Helicity (MH) states, where the magnetic fluctuations spatial spectrum is composed by many  $m=0$  and  $m=1$  modes with different toroidal mode numbers  $n$ 's and similar amplitudes. This wide  $m=1$  spectrum induces in the MH states a stochastic magnetic fields, while in QSH orderly helical flux surfaces are present in the plasma core.

The purpose of this paper is to present some experimental investigations on the thermal properties of QSH states.

### 2. Experimental set-up

The descriptions of the QSH states, and their identification, has been carried out with a complete set of diagnostics, in particular a SXR emission tomography [3, 4] and a multipoint Thomson scattering [5].

The tomographic diagnostic permits the reconstruction, with good spatial and high time resolution, of the plasma SXR emissivity  $\epsilon$  (defined as the power emitted per unit volume). The diagnostic has 78 lines of sight, with impact parameter  $p$  exceeding 0.9. The reconstruction technique is based on the truncated Fourier-Bessel expansion [6]; the inversion of the resulting matrix equations is regularised by means of the Generalised Cross Validation technique [7].

The Thomson Scattering (TS) is used for the simultaneous measurements of the electron temperature  $T_e$  and density  $n_e$  profiles. The measurements are performed along an equatorial plane from  $r/a=-0.94$  to  $r/a=0.84$ , with 2.4 cm spatial resolution. The diagnostic has been calibrated against a known light source scanning all positions so that it provides evaluation of the relative density profiles. Their shapes are generally in agreement with the density profiles measured by the multichord interferometer [8].

### 3. Electron temperature and pressure profiles in QSH states

During standard operation (MH states) the  $T_e$  profile is fairly flat in the core ( $|r/a| \leq 0.5 \div 0.6$ ) [9], the density is flat as well or slightly hollow and the reconstructed SXR emissivity profiles have the typical bell-shaped form.

On the contrary, in QSH states, together with the appearance of a  $m=1$  dominant mode in

the magnetic spectrum, the temperature and SXR profiles become asymmetric. When the helical  $m=1$  structure is measured from the tomography (see Fig. 1–a), a poloidal asymmetry is observed in the electron temperature profile (Fig. 1–b). The poloidal position of the electron temperature profile perturbation is consistent with that of the helical structure at the TS toroidal measuring station ( $\phi=82^\circ$ , which differs from that of the tomography,  $\phi=202^\circ$ ), as deduced from tomographic and magnetic measurements [10]. The electron density profile does not seem to be modified during QSH states (Fig. 1–c), even if the larger uncertainty associated with this measurement suggest that further investigation is needed to draw definite conclusions on this subject. The pressure profile is shown in Fig. 1–d and indicates that the thermal content of the helical structure is increased. Since

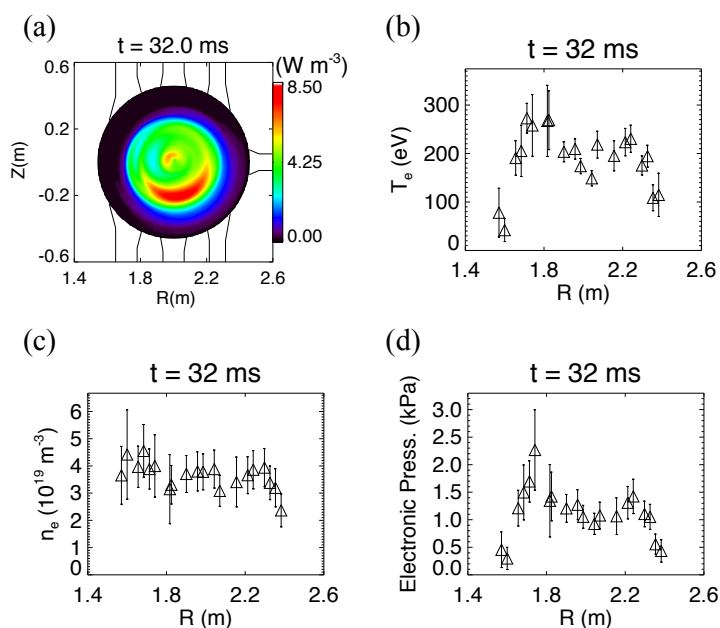


Fig. 1 (a) Contour plot of the reconstructed SXR emissivity, (b) electron temperature, (c) density and (d) pressure profile measured with the TS for a QSH shot (#12820).

there is no evidence of impurity accumulation in the centre or of a strong plasma rotation, the enhanced SXR emissivity can be ascribed to the  $T_e$  local increment and this corresponds to an improved energy content in the  $m=1$  structure. The heating of the helical structure is due to the generation of nested closed flux surfaces in it and a reduction of the level of magnetic chaos [11].

The high spatial resolution of the TS profile allows a rather high accuracy in the imaging of the electron temperature profile inside the helical structure, as shown in

Fig. 2. In this figure three different  $T_e$  profile are shown, for shots where the magnetic measurements indicated a  $m=1$  dominant mode with  $n=7$  (Fig. 2–a),  $n=8$  (Fig. 2–b) and  $n=9$  (Fig. 2–c). For each shot the contour plot of the reconstructed SXR emissivity is plotted (Fig. 2–d,e,f); the arrows indicate the position of the equatorial plane at the toroidal location of the TS, rotated to take into account the different toroidal angle of the SXR tomography. The three cases differ also for the poloidal position of the helical structure. In particular, for the profile shown in Fig. 2–a, this position at the TS toroidal location is  $\theta=220^\circ$ , in Fig. 2–b  $\theta=27^\circ$  and in Fig. 2–c  $\theta=80^\circ$ . This structure is well approximated by the temperature profile measurements: in general a single local maximum in the profile is observed, compatible with the corresponding poloidal angle  $\theta$ . Moreover, the radial location of the maximum is larger in case (c) than in (a), in agreement with the larger resonance radius of the  $n=9$  mode with respect to the  $n=7$ ; on the other hand, the temperature profiles indicate that the radial width of the structure decrease with increasing  $n$ , a result to be compared with the analogous reduction of the width of the SXR island [2].

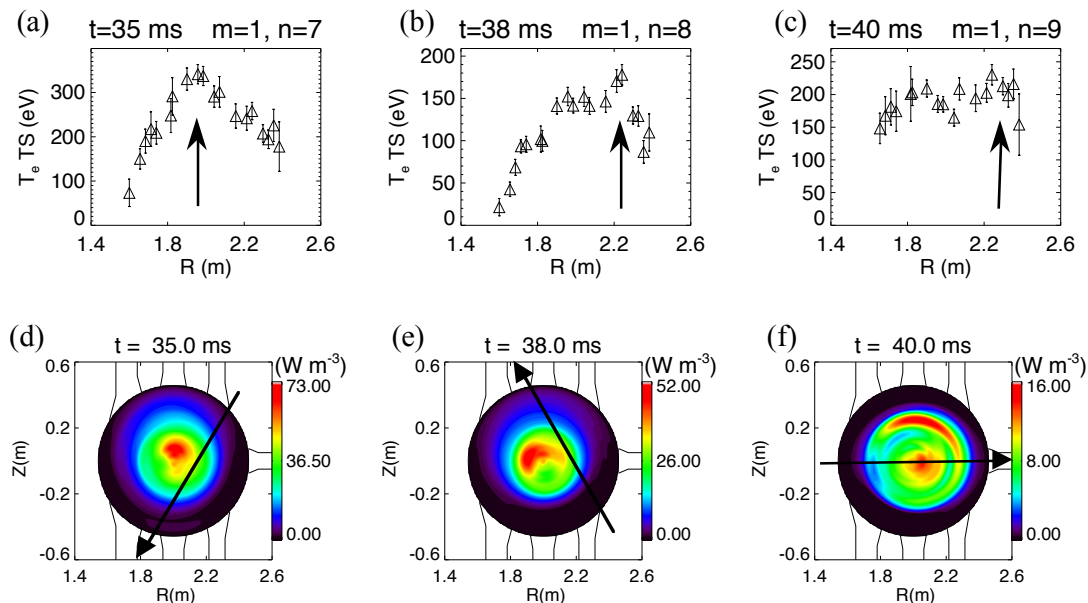


Fig. 2 Electron temperature profile for three QSH shots with (a)  $n=7$ , (b)  $n=8$  and (c)  $n=9$ ,  $m=1$  dominant mode. The position of the hot structure depends on the poloidal angle of the  $m=1$  mode. In (d), (e) and (f) the contour plot of the SXR emissivity for the three shots (same time) are plotted. The arrows indicate the position of the equatorial plane at the toroidal location of the TS seen by the SXR tomography.

#### 4. Thermal properties of the QSH

In order to characterise the energy content in the hot structure, an evaluation of the difference between the electron temperature inside and outside the island has been performed. These are plotted in Fig. 3, as a function of the number  $n$  of the dominant  $m=1$  mode. The differences

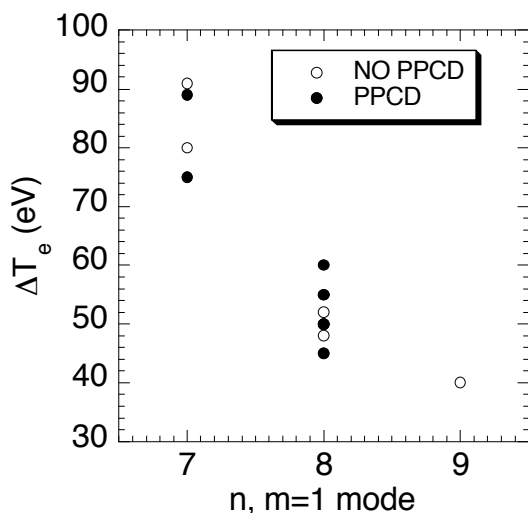


Fig. 3 Differences between the electron temperature inside and outside the hot structure, plotted as a function of the number  $n$  of the  $m=1$  dominant mode for shots with and without PPCD.

are calculated either in stationary and PPCD shots: Pulse Poloidal Current Drive is an experimental technique to drive inductively poloidal currents in the plasma in order to alleviate the need of the dynamo field and mitigate the stochasticity [12, 13]. We observe a reduction of the variation of the  $T_e$  with increasing values of  $n$ ; as previously stated, the radial width of the helical structure decreases too as  $n$  increases [2]. These two results show that the larger is the structure (more input power is deposited inside the structure) the greater is the increase of the electron temperature with respect to the remaining plasma. Fig. 3 shows

also that the variation of  $T_e$  is independent from the application of the PPCD.

Estimations of the local heat conductivity have been performed in order to obtain a rough estimate of the change of transport in the core. To do this a 1-D steady state power balance equation is applied. We have assumed that the current density  $J_{hot}$  flowing along the structure is constant and the absolute value of  $J_{hot}^2$  is considered equal to the on axis one,  $J(0)^2$ , estimated by means of the equilibrium model  $\mu&p$  [14]. The resistivity is assumed to follow the classical Spitzer formula. Supposing that the power input  $P_{in}$  flows uniformly out of the structure, the heat flux  $q$  is calculated with

$$(1) \quad q = \frac{P_{in}}{S_{hot}},$$

where  $S_{hot}$  is the structure surface. The temperature gradient scale length  $L_T$  can be defined as the average radial distance between the 75% and the 25% contours of the hot structure in the SXR emissivity, and the conductivity is given by the following:

$$(2) \quad \chi_{eff} = \frac{q}{n_e (\nabla T_e / L_T)}.$$

We obtain values of the local electron heat conductivity  $\chi_{eff}$  in the hot structure region that, in the best cases, are of the order of 60 m<sup>2</sup>/s, comparable to those obtained in PPCD shots [13].

## 5. Conclusions

During QSH states hot structures build up in the plasma core: the SXR tomography allows the imaging of these regions and the TS diagnostic gives  $T_e$  and  $n_e$  inside the structures. Thomson Scattering, tomography and magnetic diagnostics concurrently indicate the growth of a poloidally localised hot region. The observed thermal behaviour during QSH states can be interpreted as a better energy content in the structure; this is consistent with the observation that there are no particle sources and that the density profiles are rather flat in the core region. The increase of temperature in the helical region is greater for  $m=1$  mode with lower  $n$  number.

---

## References

- [1] G. Rostagni, *Fus. Eng. Design* **25** 301 (1995).
- [2] P. Martin, *et al.*, *Physics of Plasmas* **7** 1984 (2000)
- [3] P. Martin, A. Murari. *et al.*, *Rev. Sci. Instr.* **68** 1256 (1997).
- [4] A. Murari, *et al.*, in *Proceedings of the 26<sup>th</sup> EPS Conference on Controlled Fusion and Plasma Physics*, Maastricht, The Netherlands, ECA Vol. **23J** 1129 (1999).
- [5] R. Pasqualotto, A. Sardella. *et al.*, *Rev. Sci. Instr.* **70** 1416 (1999).
- [6] A. M. Cormack, *J. Appl. Phys.* **34** 2722 (1963).
- [7] N. Iwama, *et al.*, *Appl. Phys. Lett.* **54** 502 (1989).
- [8] P. Innocente, *et al.*, *Rev. Sci. Instr.* **68** 761 (1997).
- [9] A. Intravaia, L. Marrelli, P. Martin, R. Pasqualotto, *et al.*, *Phys. Rev. Lett.* **83** 5499 (1999)
- [10] P. Zanca, S. Martini, *Plasma Phys. Contr. Fusion* **41** 1251 (1999).
- [11] D. Escande, *Invited Talk*, This Conference
- [12] J. S. Sarff, N. E. Lanier, S. C. Prager and M. R. Stoneking, *Phys. Rev. Lett.* **78** 62 (1997)
- [13] R. Bartiromo, *et al.*, *Phys. Rev. Lett.* **82** 1462 (1999)
- [14] S. Ortolani, D. D. Schnack, *Magnetohydrodynamics of Plasma Relaxation*, World Scientific, Singapore, 1993